JOURNAL OF APPLIED ELECTROCHEMISTRY 1 (1971) 127–136

Screening of manganese dioxides for battery activity by thermogravimetric analysis

D. S. FREEMAN, P. F. PELTER, F. L. TYE, L. L. WOOD

The Ever Ready Co. (Great Britain) Ltd., Central Laboratories, London, U.K.

Received 8 January 1971

Manganese dioxides which are suitable as cathodes for Leclanché cells need (*a*) a high MnO_2 content and (*b*) battery activity. In this study it is shown that thermogravimetric analysis is a valuable method of screening manganese dioxides for battery activity. The parameter used is the temperature, under standard conditions, at which the rate of decomposition to Mn_2O_3 is maximum. This is called peak decomposition temperature.

Battery activity, which was assessed from actual battery discharges, correlated well with peak decomposition temperature for the 20 manganese dioxides examined. A low peak decomposition temperature indicates high battery activity.

As the total range of peak decomposition temperatures is only about 130°C, it is essential that the standard conditions are chosen to ensure decomposition of any one material over a narrow temperature range. For this reason the effects on sharpness of decomposition of gaseous environment, rate of gas flow, sample weight, particle size and rate of temperature rise have been examined. A significant improvement was effected by the use of an oxygen rather than a nitrogen environment.

Introduction

Manganese dioxides from different sources show wide variations in their performance as cathodes in Leclanché cells. A high manganese dioxide content is necessary but this alone is not sufficient and samples of acceptable chemical composition need additional testing for battery activity. Of the methods proposed for screening, X-ray diffraction has proved reliable. Poorly crystalline γ and ρ manganese dioxides usually exhibit greater battery activity than crystalline β specimens.

Even within the battery active class there are considerable differences in performance on some discharges and in general these differences have not been correlated with X-ray diffraction patterns. An exception is the performance of the narrow sub-class of electrodeposited manganese dioxides on a simulated motor discharge [1]. X-ray diffraction is not reliable in detecting minority constituents or in quantitatively analysing physical mixtures of manganese dioxides [2]. X-ray diffraction is empirical in that its relationship to battery activity is not well understood. In this situation there is need for an additional method, even if also empirical, to confirm and complement the findings of X-ray diffraction.

Thermal analysis has been used extensively in mineralogical and other studies of manganese oxides. Differential thermal analysis [2–28] and thermogravimetric analysis [23–38] have both been employed. These are dynamic techniques and hence the thermograms obtained depend upon the precise conditions and environment employed [39, 40]. Little is thus gained by careful comparison of previously published thermograms. However, some investigators have examined more than one type of manganese dioxide [2, 4–6, 10, 14, 19, 21–23, 30]. From these data there are distinct indications that the tempera-

ture at which MnO_2 decomposes to Mn_2O_3 is variable and increases in the order, electrodeposited MnO_2 and activated ores < battery active $\rho(\gamma)$ ores < pyrolusitic β ores. Only Fishburn and Dill [2] have emphasized this order as a means of classifying manganese dioxides. To the authors' knowledge no one has directly established whether there is any correlation between decomposition temperature and battery activity.

Although the decomposition temperature appears to be variable the range is only 100–150°C for the various varieties (with the possible exception of α-types which may require much higher temperatures). Thus if the technique is to have useful resolution the conditions under which any one manganese dioxide decomposes over a small temperature range must be established. Neither this aspect nor the reproducibility of decomposition temperature has received previous attention.

Thermogravimetric analysis was used in the present work and the purpose was to establish the conditions necessary for sharp decompositions, to examine reproducibility, and using conditions established to investigate various manganese dioxides and so determine whether the technique leads to a classification which is usefully indicative of battery activity.

Experimental

Apparatus

A Stanton TR-01 thermobalance fitted with the silica sheath (Part No. OS9) for controlled atmospheres was used. A flowmeter of Quickfit and Quartz design (EMO/S, 1963) with dibutyl phthalate as manometric fluid measured the constant flow of gas into the silica sheath. The sample, which was gently tapped, was contained in an alumina crucible of internal diameters 5 mm (bottom) and 13 mm (top), of wall thickness 2 mm and height 20 mm.

Temperature was measured by a Pt/13% Rh, Pt thermocouple situated with its tip touching the furnace wall at a point level with the bottom of the crucible. Experience showed that reproducible thermograms were obtained only if the thermocouple was always located in the same position.

Prior to each run the control circuits of the thermobalance were allowed to warm up for 1 h and the temperature recording pen carefully adjusted to the 20°C chart line. The speed of the chart on which sample weight and temperature were recorded was 150 mm h^{-1} up to 500°C and 600 mm h^{-1} above 500°C where the major weight changes occurred. Weight loss traces were converted to derivative curves by clamping the charts in a fixed planar orientation and a sliding adjustable protractor of 150 mm radius was used to measure slope to 0·1°.

Derivative thermograms were drawn as plots of rate of weight loss, expressed as a percentage of the original sample weight, per °C against temperature. From them we obtained (*a*) the temperature at which maximum rate of weight loss occurred (peak decomposition temperature), (*b*) the maximum rate of weight loss (peak decomposition rate) and (*c*) the width of the decomposition band in °C at half the peak decomposition rate (decomposition band width). The major information is peak decomposition temperature; peak decomposition rate and decomposition band width are secondary but useful in assessing the sharpness of decomposition. Although peak decomposition temperature has less significance than the temperature at which decomposition commences the former is more readily located, particularly for manganese dioxides where the onset of decomposition is blurred by water loss, and is preferred. The temperature is not the temperature of the sample but of the thermocouple tip at the furnace wall and in this sense it is unlikely that our data could be exactly reproduced elsewhere. The objects of the study are relative not absolute so this limitation is not regarded as serious.

Programme

The effects of thermograms of the following variables were investigated:

(*a*) Gaseous environment. Oxygen at 4 l h^{-1}, nitrogen at 4 l h^{-1}.
(*b*) Rate of gas flow. Oxygen at 1, 2, and 4 l h^{-1}.
(*c*) Sample weight, 0·5 and 0·05 g.
(*d*) Particle size. Fractions (B.S.S.) −25+36, −60+100, −150+200, and 80% −200.

Table 1. Analysis and crystallinity

Code	*Type of material*	*Description*	*Crystallinity*	*x in* MnO_x	MnO_x (%)	H_2O (110°C) (%)	*Combined* H_2O (%)
R32	Electrodeposit	Source D	γ	1·972	92·4	1·75	2·79
R9	Electrodeposit	Source C	γ	1·959	91·2	2·63	3·40
R6	Electrodeposit	Source B	γ	1·970	92·5	2·12	2·92
R2	Electrodeposit	Source A	γ	1·951	93·4	1·59	4·33
S1	Chemical	Faradiser M	γ	1·946	94·0	2·43	2·70
R16	Electrodeposit	Source E	γ	1·940	91·5	2·01	2·68
R18	Activated ore	Ergogene	γ, β	1·932	83·4	1·85	2·50
S3	Activated ore	Experimental	ρ	1·913	85·4	1·18	
R10	Activated ore	Ever Ready	γ	1·939	85·6	3·07	3·47
R1	Ore	Ghana D	ρ	1·956	88·7	0·51	3·23
R15	Ore	Gabon	ρ	1·962	87·2	0·76	3·71
R19	Ore	Montana	ρ	1·925	69·9	2·35	3·70
R7	Ore	Chinese	ρ, β	1·905	93·0	0·78	2·06
R3	Ore	South African	ρ	1·953	76·3	1·14	3·94
R14	Ore	Greek	ρ	1·952	74·9	1·65	3·67
R25	Chemical	Boots	δ	1·984	73·5	10·63	6·58
R5	Ore	Botswana	β, ρ	1·946	72·9	0·67	3·23
R30	Ore	Caucasian	β	1·992	89·8	0·71	1·75
R20	Ore	Moroccan	β	1·987	94·4	0·18	0·86
S2	Ore	Turkish	β	1·987	92·6	0·46	
R26	Ore	Sinai	β	1·991	87·4	0·57	1·15
R24	Ore	Spanish	β	1·975	80·8	1·13	2·11

(*e*) Rate of temperature rise. 20 to 1000°C in 4, 6, 8, 12, 16, and 24 h.

From this work standard conditions were chosen and used to check reproducibility and to obtain the thermograms of twenty-two manganese dioxides.

Materials

The manganese dioxides used are listed in Table 1 together with analytical data and crystallinity designations. They were powders with at least 80% passing through B.S.S. 200. The only exceptions were the samples used to ascertain the effect of particle size.

Only the main crystalline phases in order of preponderance are noted in Table 1. With many of the samples there were small amounts of other phases also present, e.g. β phase in some electrodeposited manganese dioxides [1]. Crystallinity designations were deduced from X-ray diffractions of the powders obtained with a Philips PW 1130/00 diffraction generator/PW 1050/25 goniometer and PW 1965/30 proportional detector connected to a PW 1360/00 recording assembly and using Cu radiation with Ni filter at a current of 40 mA and a potential of 45 kV.

Analytical determinations were as follows: manganese by potentiometric titration with potassium permanganate [41], available (active) oxygen by the oxalate method [42] modified by addition of $Fe^{3(+)}$ to prevent catalytic decomposition by $Mn^{2(+)}$ [43], H_2O (110°C) by heating at 110°C for three periods of 4 h with intermediate weighing, total water by heating at 1000°C for 1 h in a stream of dry oxygen and weighing the evolved water after absorption on magnesium perchlorate. Combined water was calculated from total water by subtracting H_2O (110°C).

Where the sample for thermogravimetric analysis was from a different batch to that analysed, an asterisk is added to the code number.

Battery activity

This will be reported in detail elsewhere. For our present purpose it is sufficient to note that for

every manganese dioxide, individual R20 size cells of paper-lined construction were made each containing 23·08 g of the manganese dioxide [1]. The cells were discharged at 20°C, 7 days per week on five different regimes representing a range of applications:

(*i*) through 40 ohms for 4 h per day to an endpoint (on load) of 0·9 V [44];
(*ii*) through 5 ohms for 30 m per day to an endpoint (on load) of 0·75 V [44];
(*iii*) through 2·5 ohms for 10 m per day to an endpoint (on load) of 0·9 V;
(*iv*) through 5 ohms for 2 h per day to an endpoint (on load) of 1·1 V;
(*v*) through 1·5 ohms for 10 m per day to an endpoint (on load) of 1·0 V.

On each regime, discharge lives were expressed as a percentage of the maximum life obtained for the twenty-two materials. A manganese dioxide was considered active on a regime if it had a discharge life of at least 60% of the maximum discharge life obtained. Battery activity is then indicated by the number of regimes on which the material was found active. For example, battery activity 4 indicates that on four of the five discharge regimes the manganese dioxide showed a discharge life of at least 60% of the best performing manganese dioxide.

Results and Discussion

Environment

Table 2 shows the effect of gaseous environment.

Decomposition in oxygen occurred at a higher temperature than in nitrogen. Hegedus [37] has made a similar observation and Matsushima and Thoburn [20] have shown that decomposition moves to higher temperatures with increase in oxygen pressure. Of more import in the present context is the higher peak decomposition rate and smaller decomposition band width found in oxygen. Fig. 1 compares the decomposition of Ghana ore in oxygen and nitrogen.

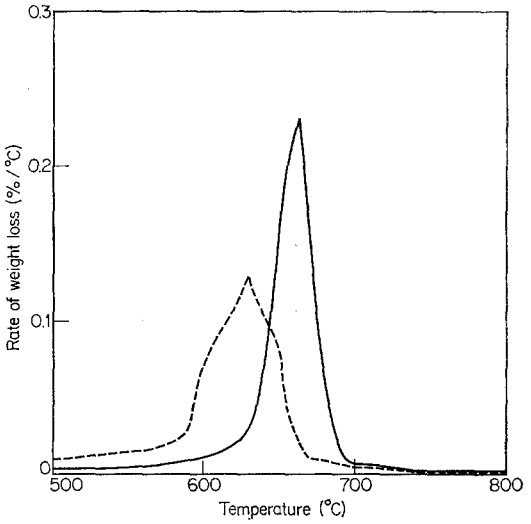

Fig. 1. Derivative thermograms of Ghana ore (R1)
– – – – in nitrogen
——— in oxygen.

The shift to higher temperatures and the increase in sharpness of some decompositions when carried out in an atmosphere of the evolved gas is known and Garn [45] has given an excellent account of the underlying reasons for this behaviour. It is a consequence of the reversi-

Table 2. Effect of gaseous environment
(Rate of gas flow 4 l h^{-1}, sample weight 0·5 g, rate of temperature rise 20–1,000°C linearly in 4 h.)

Code	*Peak decomposition temp (°C)*		*Peak decomposition rate (%/°C)*		*Decomposition band width (°C)*	
	Oxygen	*Nitrogen*	*Oxygen*	*Nitrogen*	*Oxygen*	*Nitrogen*
R2	619	594	0·32	0·19	21	36
R6	618	592	0·21	0·12	32	52
R16	632	588	0·28	0·12	24	50
R1	662	630	0·23	0·13	28	52
R15	675	620	0·20	0·09	29	60
R30	722	690	0·19	0·12	32	56

Table 3. Effect of oxygen flow rate
(Sample R16*, sample weight 0·5 g, rate of temperature rise 20–1000°C linearly in 4 h.)

Rate of gas flow (1 h^{-1})	1	2	4
Peak decomposition temperature (°C)	600	600	600
Peak decomposition rate (%/°C)	0·28	0·26	0·29
Decomposition band width (°C)	32	34	25

bility, or at least partial reversibility, of the decomposition and the law of mass action.

Reversibility is the reason why oxygen is an unsuitable environment in which to examine partially reduced manganese dioxides [35, 36]. Our concern is, however, with manganese dioxides that are essentially unreduced and for these it is clear that an oxygen environment is preferable if sharp decompositions are required.

Rate of gas flow

To maintain a particular gaseous environment it was necessary to flow gas past the sample. Newkirk [46] has shown that this can cause errors. However, Table 3 demonstrates that there was no significant effect on peak decomposition temperature or on sharpness of decomposition for oxygen flow rates in the range 1 to 4 l h^{-1}.

Sample weight

It would seem desirable to use the thermobalance near its maximum capability. The maximum weight loss that could be accommodated automatically was 0·095 g. The maximum weight loss expected from a manganese dioxide was 16%; 9·2% for the decomposition MnO_2 to Mn_2O_3, and 6·8% water loss (Table 1). The sample weight must be less than 0·59 g if a weight loss of 16% was to be less than 0·095 g. Thus a sample weight of 0·5 g was near to the maximum capability of the thermobalance. Under these conditions the buoyancy correction was insignificant. (Abnormal materials such as R25 which has a water content of 17% were accommodated by a manual weight addition to the sample side during the run.)

Table 4 compares thermograms for sample weights of 0·50 g and 0·05 g and shows that there is no substantial difference in the sharpness of decomposition. Hegedus [37] has previously noted no difference in the rate of thermal decomposition of β MnO_2 with different sample weights.

Particle size

Table 5 shows that for one sample, particle size had no effect on peak decomposition or on sharpness of decomposition. This would be expected for a reversible decomposition taking place in a constant environment of the evolved gas. In such circumstances the decomposition would be controlled only by equilibrium constants and the pressure of the evolved gas.

If kinetics or diffusion exerted an influence on the decomposition some dependence on surface area might be expected. Manganese dioxides are

Table 4. Effect of sample weight
(Sample R16*, gaseous environment oxygen, rate of gas flow 4 l h^{-1}, rate of temperature rise 20–1000°C linearly in 4 h.)

Sample weight (g)	*Peak decomposition temp. (°C)*	*Peak decomposition rate (%/°C)*	*Decomposition band width (°C)*
0·50	600	0·29	25
0·05	605	0·34	20

Table 5. Effect of particle size
(Gaseous environment oxygen, rate of gas flow 4 l h^{-1}, sample weight 0·5 g, rate of temperature rise 20–1000°C linearly in 4 h.

Particle size (B.S.S.)	*Sample*	*Peak decomposition temp. (°C)*	*Peak decomposition rate (%/°C)*	*Decomposition band width (°C)*
80%−200	R3	680	0·13	34
−150+200	R3*	698	0·14	30
−60+100	R3*	678	0·13	24
−25+36	R3*	678	0·13	32

usually of sufficient porosity [47–49] that the surface is predominantly internal and so again particle size should be unimportant.

Rate of temperature rise

Table 6 shows that peak decomposition temperature decreased and that sharpness of decomposition increased a little as the rate of temperature rise decreased. The former effect is attributed to a smaller temperature lag between the sample and the temperature recorded at the furnace wall and the latter to improved temperature homogeneity in the sample as the rate of temperature rise decreased.

It was judged that the improvement in decomposition sharpness was not sufficient to outweigh the convenience of being able to carry out two 4 h runs in a normal working day.

Standard conditions and reproducibility

The standard conditions chosen on the basis of the foregoing experiments are shown in Table 7.

Using the standard conditions, replicate runs were carried out on five manganese dioxides. The values obtained for peak decomposition temperature, peak decomposition rate and decomposition band width are given in Tables 8, 9 and 10 respectively.

Analysis of variance [50] of the data yields estimates of 'within groups' means squares from which standard deviations of 4·3°C, 0·013%/°C and 2·7°C are obtained for peak decomposition temperature, peak decomposition rate and decomposition band width respectively. It follows that when a single run is made there is a 95% probability that the values obtained for peak decomposition temperature, peak decomposition rate and decomposition band width will be respectively within 9·2°C, 0·028%/°C and and 5·7°C of the true means.

Thus the precision with which peak decomposition temperature can be determined is quite good and adequate to differentiate materials whose peak decomposition temperatures vary over a 130°C range. Peak decomposition rate and decomposition band width are less reproducible

Table 6. Rate of temperature rise
(Gaseous environment oxygen, rate of gas flow 4 l h^{-1}, sample weight (*a*) 0·5 g, (*b*) 0·1 g.)

Linear rise time 20–1,000°C (h)	*Peak decomposition temp. (°C)*		*Peak decomposition rate (%/°C)*		*Decomposition band width (°C)*	
	R16*	R20*	R16*	R20*	R16*	R20*
4[a]	600	720	0·29	0·18	25	46
6[a]	598		0·29		24	
8[b]	595		0·32		20	
12[a]		692		0·22		28
16[b]	578		0·36		18	
24[a]	576	692	0·36	0·25	18	20

Table 7. Standard thermogravimetric analysis conditions

Gaseous environment	Oxygen
Rate of gas flow	4 l h^{-1}
Sample weight	0·5 g
Particle size	>80% through B.S.S. 200
Rate of temperature rise	20–1000°C linearly in 4h

Table 8. Replicate values of peak decomposition temperature

Material code	*Peak decomposition temperature (°C)*
R1	654, 660, 660, 662, 668, 668
R2	616, 618, 618, 620, 622, 624
R14	698, 702, 704
R15	670, 678, 678
R16	628, 632, 638

Table 9. Replicate values of peak decomposition rate

Material code	*Peak decomposition rate (%/°C)*
R1	0·23, 0·22, 0·24, 0·24, 0·22, 0·26
R2	0·31, 0·32, 0·33, 0·31, 0·35, 0·32
R14	0·14, 0·14, 0·14
R15	0·21, 0·20, 0·18
R16	0·27, 0·28, 0·28

Table 10. Replicate values of decomposition band width

Material code	*Decomposition band width (°C)*
R1	26, 30, 28, 26, 30, 28
R2	24, 20, 22, 16, 20, 24
R14	30, 24, 30
R15	30, 26, 32
R16	26, 22, 26

but are still sufficiently precise for comparisons to be of value.

Comparison of manganese dioxides

Thermogravimetric data using the standard conditions, battery activity and the crystallinity designations of the various manganese dioxides are compared in Table 11. Where two peaks or a peak and a shoulder were observed the temperature of the predominant peak is given first. Figures for shoulders are in brackets. Peak decomposition rates are for the predominant peaks.

Table 11. Thermogravimetric data and battery activity

Code	*Type of material*	*Description*	*Crystallinity*	*Battery activity*	*Peak decomposition temp. (°C)*	*Peak decomposition rate (%/°C)*	*Decomposition band width (°C)*
R32	Electrodeposit	Source D	γ	5	610	0·18	38
R9	Electrodeposit	Source C	γ	5	618	0·17	26
R6	Electrodeposit	Source B	γ	5	618	0·21	32
R2	Electrodeposit	Source A	γ	5	619	0·32	21
S1	Chemical	Faradiser M	γ	5	620	0·19	22
R16	Electrodeposit	Source E	γ	5	632	0·28	24
R18	Activated ore	Ergogene	γ, β	4	626 (632)	0·10	40
S3	Activated ore	Experimental	ρ		628	0·18	32
R10	Activated ore	Ever Ready	γ	4	634	0·16	30
R1	Ore	Ghana D	ρ	3	662	0·23	28
R15	Ore	Gabon	ρ	3	675	0·20	29
R19	Ore	Montana	ρ	3	675	0·06	56
R7	Ore	Chinese	ρ, β	3	682 (672)	0·11	50
R3	Ore	South African	ρ	2	680	0·13	34
R14	Ore	Greek	ρ	2	701	0·14	28
R25	Chemical	Boots	δ	2	see text		
R5	Ore	Botswana	β, ρ	1	704, 678	0·08	66
R30	Ore	Caucasian	β	1	722	0·19	32
R20	Ore	Moroccan	β	0	700	0·17	48
S2	Ore	Turkish	β		726	0·25	32
R26	Ore	Sinai	β	0	728	0·21	36
R24	Ore	Spanish	β	0	736	0·22	26

Battery activity will be discussed fully elsewhere. It is sufficient here, to note that all categories of battery activity from 0 to 5 are covered and to recall that the battery activities are based directly on the actual performance of batteries rather than on one of the many laboratory assessment procedures.

The important result is the good correlation between battery activity and peak decomposition temperature. The peak decomposition temperature of synthetic materials and activated ores with battery activities of 4 and 5 is below 645°C. For active ores with battery activities of 2 and 3 the peak decomposition temperature is between 645 and 700°C, while for inactive ores with battery activities of 0 and 1 the peak decomposition temperature is above 700°C.

Further subdivision as shown in Table 12 may be possible although more samples would be necessary to confirm such an exact correlation between battery activity and peak decomposition temperature.

A good correlation between peak decomposition temperature and crystalline type is also evident from Table 11. Peak decomposition temperatures of 645 and 700°C again provide boundary points, in this case dividing γ, ρ and β crystalline phases. This confirms the findings of Fishburn and Dill [2] and refutes the suggestion of Glemser, Gattow and Meisiek [26] that thermogravimetric analysis cannot differentiate manganese dioxide modifications.

Except for R19 and R20, manganese dioxides which by X-ray diffraction are essentially of one crystalline type, show peak decomposition rates of 0·13 to 0·32%/°C and decomposition band widths of 21 to 38°C. These ranges and particularly that for peak decomposition rate are greater than is expected from normal experimental variation and therefore particular values have significance. There is no correlation with battery activity or crystalline type. It is possible that particularly sharp decompositions, e.g. R2, may indicate greater crystalline purity and broader decompositions, e.g. R3, the converse. The very broad decomposition observed with R19 certainly suggests the presence of more than one crystalline type and some α material is detectable in the X-ray pattern.

Table 12. Correlation of battery activity and peak decomposition temperature

Class of material	*Battery activity*	*Peak decomposition temp. (°C)*
Active synthetic	5	600–625
Activated ore	4	625–645
Very active ore	3	645–680
Active ore	2	680–700
Inactive ore	1, 0	700–740

On the other hand R20, for which the decomposition was also broad, showed only β crystallinity. The X-ray lines were very sharp [47] indicating large crystallite size. Relative to other manganese dioxides, Moroccan ore (R20) exhibits less ion-exchange [47] and lower internal pore volume [47]. These facts all suggest low surface area and hence the broad decomposition may in this case be due to kinetic or diffusion restrictions. It is interesting that at slower rates of temperature rise, which minimize kinetic and diffusion effects, the decomposition band width of R20 was not significantly greater than that of R16 which was one of the sharper decomposing manganese dioxides (see Table 6).

There were two main crystalline phases in three of the manganese dioxides investigated (R5, R7 and R18). These materials had two peaks (R5) or a main peak and a shoulder (R7 and R18). The decompositions were broad with peak decomposition rate less than 0·12%/°C and decomposition band width 40°C or greater.

The derivative thermograms of three manganese dioxides of essentially single crystalline type which are reasonably typical of the battery active classes 5/4, 3/2 and 1/0 are compared in Fig. 2. Their shapes are similar and are only distinguished by their different positions on the temperature axis. This indicates that the different peak decomposition temperatures are largely the result of different thermal stabilities rather than due to diffusion or kinetic effects. This is consistent with the concept of a reversible (or partially reversible) decomposition which has been invoked to explain the effect of gaseous environment.

One manganese dioxide, R25, gave a thermogram (Fig. 3) which was quite unlike any other. The material was chemically precipitated and of

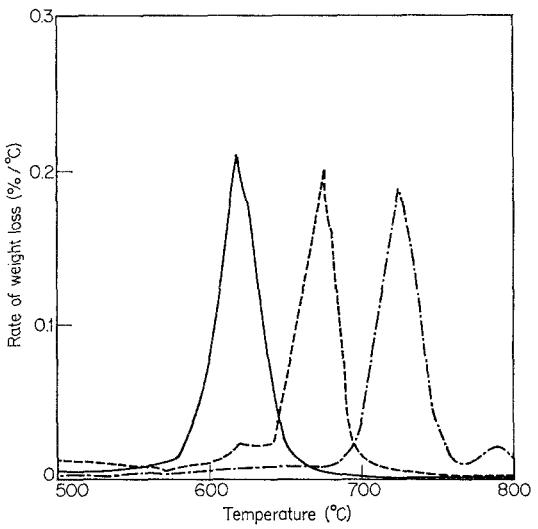

Fig. 2. Comparison of derivative thermograms
——— very active synthetic material (R6)
– – – – active ore (R15)
— · — inactive ore (R30).

abnormally high water content. A weight loss equivalent to the water content was obtained up to 340°C. No weight loss was observed between 500 and 780°C where decomposition would normally be expected. The weight loss between 340 and 1000°C was equivalent to decomposition of 46% of original manganese dioxide. At 1000°C the gas stream was switched to nitrogen and decomposition equivalent to a further 44% of the manganese dioxide occurred. The material contained 4% potassium and it was possible that on heating a stable α form was produced.

Conclusion

Peak decomposition temperature correlates well with battery activity and can be determined with adequate precision. A low peak decomposition temperature indicates high battery activity.

Thermogravimetric analysis is thus a valuable technique for screening manganese dioxide samples for battery activity.

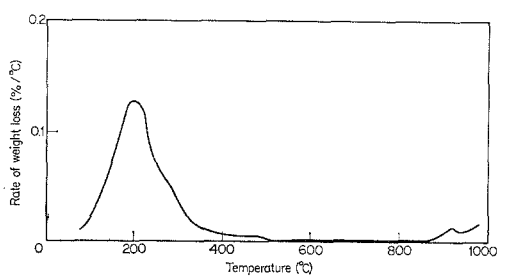

Fig. 3. Derivative thermogram of R25.

Acknowledgments

The authors thank the Directors of The Ever Ready Company (G.B.) Limited for permission to publish the paper, M. G. Allen for careful checking of the primary data, and J. H. J. Mallaby for advice on statistical aspects.

References

[1] A. Agopsowicz and F. L. Tye, *J. Applied Electrochem.*, **1** (1971) 45–52
[2] H. W. Fishburn and W. E. Dill, *Proc. 15th Annual Power Sources Conference*, (1961) 98.
[3] S. Pavlovitch, *Comptes rendus de L'Academie des Sciences*, **200** (1935) 71.
[4] H. F. McMurdie and E. Golovato, *J. Res. Nat. Bur. Standards*, **41** (1948) 589.
[5] I. S. Morosov and V. G. Kuznetsov, *Uzvest. Akad. Nauk SSSR., Otdel. Khim. Nauk*, (1949) p. 343.
[6] P. H. Delano, *Ind. Eng. Chem.*, **42** (1950) 523.
[7] A. J. Kauffman and E. D. Dilling, *Econ. Geology*, **45** (1950) 222.
[8] J. L. Kulp and J. N. Perfetti, *Min. Mag.*, **29** (1950) 239.
[9] H. Heystek and E. R. Schmidt, *Trans. Geological Soc., South Africa*, **LVI** (1953) 149.
[10] N. S. Krishna Prasad and C. C. Patel, *J. Indian Inst. Science*, **36** (1954) 23.
[11] P. Ljunggren, *Geologiska Foreningens Forhandlingar*, **77** (1955) 135.
[12] M. Foldvari-Vogl and V. Koblencz, *Acta Mineralogica—Petrographica*, **9** (1956) 7.
[13] M. Foldvari-Vogl and V. Koblencz, *Acta Geologica Acad. Sci. Hung.* **4** (1957) 85.
[14] A. Kozawa, *J. Electrochem Soc.*, **106** (1959) 79.
[15] N. S. Krishna Prasad and C. C. Patel, *Bull. India Electrochem. Soc.*, **12** (1963) 12.
[16] A. Regner, V. Ettel and J. Veprek-Siska, *Collection Czechoslov. Chem. Commun.* **28** (1963) 2854.
[17] A. B. Rao and V. K. Nayak, *Academia Brasileira, De Ciencias*, **35** (1963) 539.
[18] M. Fleischer and G. T. Faust, *Schweizerische Mineralogische und Petrographische Mitteilungen*, **43** (1963) 197.
[19] R. J. Ortlepp, *Trans. Proc. Geological Soc., South Africa*, **67** (1964) 149.
[20] T. Matsushima and W. J. Thoburn, *Canadian J. Chem.*, **43** (1965) 1723.
[21] H. Tamura, *Asahi Garasu Kogyo Gitjutsu Sharei-Kai Kenkyu Hokoku*, **13** (1967) 497.

[22] F. H. Gouge and R. L. Orban, *Electrochem. Technol.*, **5** (1967) 501.
[23] Y. Ukai, S. Nishimura, and T. Mayeda, *J. Mineralogical Soc. Japan*, **2** (1956) 431.
[24] M. Fleischer, *Amer. Min.*, **45** (1960) 176.
[25] S. Ghosh and J. P. Brenet, *Electrochimica Acta*, **7** (1962) 449.
[26] O. Glemser, G. Gattow, and H. Meisiek, *Z. anorg. allg. Chemie* **309** (1961) 1.
[27] C. Naganna, *Proc. Indian Acad. Sciences*, **58** (1963) 16.
[28] C. Naganna, *Acta Univ. Carolinae Geol. Monographia*, **2** (1964) 1.
[29] T. Dupuis, J. Besson, and C. Duval, *Analytica Chimica Acta*, **3** (1949) 599.
[30] J. Brenet and A. Grund, *Academic des Sciences*, (1955) 1210.
[31] G. Grasselly and E. Klivenyi, *Acta Mineralogica—Petrographica*, **9** (1956) 15.
[32] G. M. Faulring, W. K. Zwicker and W. D. Forgeng, *Amer. Min.*, **45** (1960) 946.
[33] H. Shiratori and H. Moriya, *J. Electrochem. Soc. Japan*, **29** (1961) E 134.
[34] S. Tobisawa, *Memoirs of the Defence Academy, Japan*, **2** (1963) 103.
[35] J. P. Gabano, B. Morignat, E. Fialdes, B. Emery, and J. F. Laurent, *Zeit Physik. Chem. N.F.*, **46** (1965) 359.
[36] P. Brouillet, A. Grund, F. Jolas, and R. Mellet, 'Batteries 2', Ed. D. H. Collins, Pergamon Press, London (1965) p. 189.
[37] A. J. Hegedus, *Magyar Kemiai Folyoirat*, **72** (1966) 79.
[38] J. Ambrose, A. K. Covington and H. R. Thirsk, 'Power Sources 2, 1968', Ed. D. H. Collins, Pergamon Press, London (1970) p. 303.
[39] H. G. McAdie, *Anal. Chem.*, **39** (1967) 417.
[40] P. D. Garn, 'Thermoanalytical Methods of Investigation', Academic Press, London (1965).
[41] J. J. Lingane and R. Karplus, *Analyt. Chem.*, **18** (1946) 191.
[42] F. P. Treadwell and W. T. Hall, 'Analytical Chemistry', 9th Ed., Wiley, New York (1942) p. 559.
[43] K. Sasaki and K. Ito, *J. Electrochem. Soc. Japan* (Overseas Ed.) **27** (1959) E 92.
[44] I.E.C. Pub. 86–2, Amd. 1.
[45] P. D. Garn, [40] Chapter VII.
[46] A. E. Newkirk, *Anal. Chem.*, **32** (1960) 1558.
[47] J. Muller, F. L. Tye and L. L. Wood, 'Batteries 2', Ed. D. H. Collins, Pergamon Press, London (1965) p. 201.
[48] M. A. Dakri, F. L. Tye, and J. L. Whiteman, 'Power Sources 1966', Ed. D. H. Collins, Pergamon Press, London (1967) p. 65.
[49] K. Le Tran, *J. Chim. Phys.* **64** (1967) 922.
[50] C. A. Bennett and N. L. Franklin, 'Statistical Analysis in Chemistry and Chemical Industry', John Wiley and Sons, New York (1954) p. 327.